JOURNAL OF SYNCHROTRON RADIATION

ISSN 1600-5775

A confident source of hard X-rays: radiation from a tokamak applicable for runaway electrons diagnosis

M. Kafi, A. Salar Elahi,* M. Ghoranneviss, M. R. Ghanbari and M. K. Salem

Plasma Physics Research Center, Science and Research Branch, Islamic Azad University, Tehran, Iran.
*Correspondence e-mail: salari_phy@yahoo.com

Received 14 April 2016
Accepted 24 June 2016

Edited by M. Yamamoto, RIKEN SPring-8 Center, Japan

Keywords: tokamak; runaway electrons; hard X-rays.

In a tokamak with a toroidal electric field, electrons that exceed the critical velocity are freely accelerated and can reach very high energies. These so-called 'runaway electrons' can cause severe damage to the vacuum vessel and are a dangerous source of hard X-rays. Here the effect of toroidal electric and magnetic field changes on the characteristics of runaway electrons is reported. A possible technique for runaways diagnosis is the detection of hard X-ray radiation; for this purpose, a scintillator (NaI) was used. Because of the high loop voltage at the beginning of a plasma, this investigation was carried out on toroidal electric field changes in the first 5 ms interval from the beginning of the plasma. In addition, the toroidal magnetic field was monitored for the whole discharge time. The results indicate that with increasing toroidal electric field the mean energy of runaway electrons rises, and also an increase in the toroidal magnetic field can result in a decrease in intensity of magnetohydrodynamic oscillations which means that for both conditions more of these high-energy electrons will be generated.

1. Introduction

The collisional friction force acting on an electron in a plasma increases linearly at small velocity, like in a conventional fluid or gas, but reaches a global maximum value of $f(v) = mv_{ee}(v)$ at the thermal velocity $v = v_{th}$. The collision frequency for super-thermal electrons decreases with the velocity as

$$v_{ee} = \frac{e^4 n_e \ln \Lambda}{4\pi\varepsilon_0 m_e^2 v^3}, \qquad (1)$$

where n_e is the electron density, m_e is the electron mass, e is the elementary charge and $\ln \Lambda$ is the Coulomb logarithm. Thus, in an electric field, electrons with velocity above the critical value will be accelerated continuously; in other words they 'run away' (Guan *et al.*, 2010; Helander *et al.*, 2002). Runaway electrons are often formed during disruptions. A disruption is a fast unstable event that leads to a sudden loss of plasma confinement. There are, in general, two ways of producing runaway electrons, *i.e.* primary and secondary generation. In the former, fast electrons are formed through the combined effects of a constant electric field and velocity-space diffusion. This means that thermal electrons diffuse through the high-energy tail of the thermal electron population to increasingly higher energy (Gurevich, 1961; Kruskal & Bernstein, 1962; Connor & Hastie, 1975; Cohen, 1979). In the secondary process, runaway electrons are generated due to interaction of the runaway electrons with thermal electrons (an avalanche mechanism) (Sokolov, 1979). There is experimental evidence that such secondary generation of electrons does in fact occur in non-disruptive plasma (Jaspers *et al.*, 1993). Runaway and

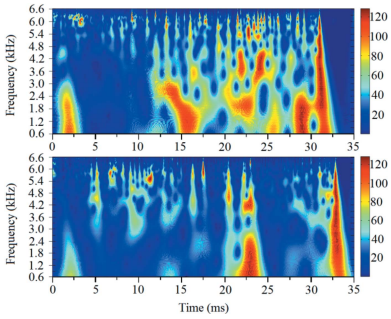

super-thermal electrons, which are produced and escape from a tokamak, can deliver information about non-linear processes occurring inside a high-temperature plasma. Such electrons can even cause very intense damage (*e.g.* erosion, melting, *etc.*) of a chamber wall, escaping in large facilities of the tokamak type (Lipa *et al.*, 2003). Runaway electrons colliding with residual plasma particles and the first wall are two sources of hard X-ray radiation in tokamaks (Naghidokht *et al.*, 2016; Salar Elahi & Ghoranneviss, 2009*a*, 2010*a*,*b*,*c*,*d*,*e*; Emami *et al.*, 2009; Ghoranneviss *et al.*, 2010; Salar Elahi *et al.*, 2009*a*). Although the intensity of radiation due to collisions with heavy nuclei of the first wall is higher, in both cases the dominant mechanism is bremsstrahlung (Salar Elahi & Ghoranneviss, 2009*b*,*c*,*d*,*e*,*f*, 2010*f*, 2014; Salar Elahi *et al.*, 2009*b*,*c*; Rahimi Rad *et al.*, 2009; Ghanbari *et al.*, 2014, 2016; Mikaili Agah *et al.*, 2015*a*,*b*). According to the bremsstrahlung mechanism most of the hard X-ray photons are emitted in a cone with a half-angle of $1/Y$ in the direction of the velocity of the emitting runaway electrons, where

$$Y = E_r\,[\mathrm{MeV}]/0.512. \quad (2)$$

Also, the energy distribution function of runaway electrons can be described by

$$E \propto \exp(-E/E_r), \quad (3)$$

where E is the energy of the hard X-ray photons and E_r is the mean energy of the runaway electrons. Therefore E_r could be deduced from the inverse slope of the energy spectrum (Emami *et al.*, 2009; Salar Elahi & Ghoranneviss, 2010*c*). The main aim of this paper is to consider the effect of a toroidal electric and magnetic field on the parameters of fast electrons in the IR-T1 tokamak. As the runaway electrons are almost collisionless, they can be affected easily by a toroidal magnetic field, so they can be used for investigating the magnetic characteristics of a tokamak plasma. Furthermore, the toroidal electric field changes on the mean energy of these high-energy electrons were studied. The importance of studying these high-energy electrons is due to their destructive characteristics, especially during the main disruption, for future fusion reactors and their plasma confinement.

2. Experimental setup

The specific characteristics of the IR-T1 tokamak, which is categorized as a small-size tokamak, are an ohmically heated air core tokamak with a major radius of R = 0.45 m and a minor radius of a = 0.125 m defined by two poloidal stainless-steel limiters. The vacuum chamber has a circular cross section with two toroidal breaks and a minor radius of b = 0.15 m. The toroidal magnetic field $B_t \simeq 0.6$–0.8 T, the plasma current $I_P \simeq$ 25–30 kA, the average electron density in hydrogen is 0.7–1.5 $\times$ 10^{19} m^{-3}, the plasma discharge duration $t_d \simeq 35$ ms and the electron temperature $T_e(0) \simeq$ 150–180 eV. The average pressure before discharge was 2.1 $\times$ 10^{-5} Torr. In this experiment, in order to detect and analyze the hard X-ray spectrum, a 2 inch $\times$ 2 inch NaI scintillator has been used (Fig. 1). The detector is located at a distance of 3–4 m from a vacuum vessel in the equatorial plane. The voltage applied to the photomultiplier was 800 V and the hard X-ray intensity in the detector can be identified on data acquisition after preamplifier and amplifier.

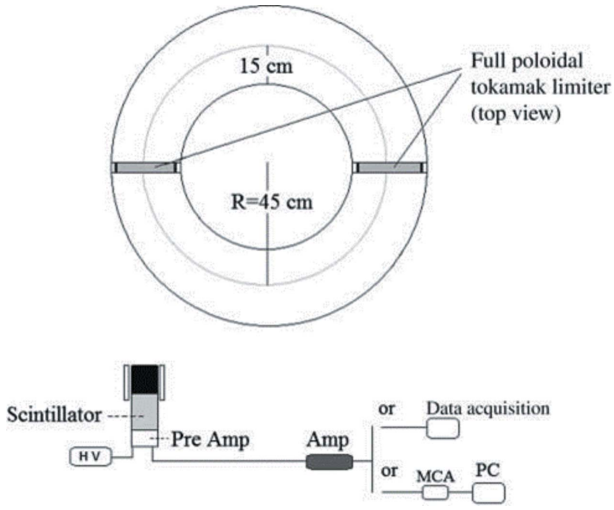

Figure 1
Schematic illustration of IR-T1 (top view) showing the hard X-ray detector system. HV: high-voltage power supply for the scintillator; Pre Amp and Amp: preamplifier and amplifier, respectively.

In order to obtain a hard X-ray spectrum (counts with respect to energy of photons), a multichannel analyzer (MCA) was used. The output signal from the detector was analyzed by the MCA and this spectrum was observed *via* computer. To obtain enough counts per channel, the MCA was set to '1024 channel' mode. Two standard Cs^{137} (0.66 MeV) and Am^{241} (59.54 MeV) sources were employed in order to calibrate the MCA.

3. Results and discussion

In this section the effect of the toroidal electric and magnetic field changes on the runaway electrons parameters is presented. The toroidal electric field was altered and the changes of the energy spectrum of the runaway electrons were observed. Figs. 2 and 3 show the plasma current, loop voltage, Mirnov oscillations and hard X-ray signal from the IR-T1 tokamak before and after increasing the toroidal electric field.

Figs. 4 and 5 show two spectra of emitted hard X-rays for two different toroidal electric fields in the first 5 ms interval, from the beginning of the plasma. This period of time is important because at that moment the loop voltage is very high and consequently more runaway electrons will be generated. The mean energy was calculated from the slope of the energy spectrum of the hard X-ray photons. Figs. 4(*a*) and 4(*b*) show curves with two slopes: the first slope is related to super-thermal electrons and the second one is related to runaway electrons. According to this investigation, with the increase of the toroidal electric field the slope related to the super-thermal electrons did not change but the mean energy of the runaway electrons increases with increasing toroidal electric field.

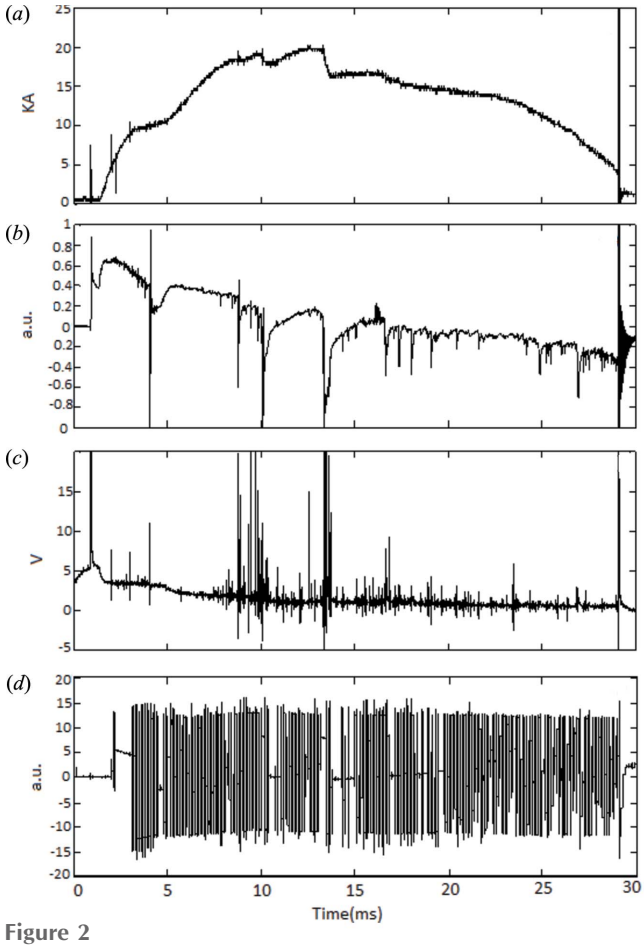

Figure 2
(*a*) Plasma current, (*b*) Mirnov oscillations, (*c*) loop voltage and (*d*) hard X-rays with respect to the time before decreasing the toroidal electric field.

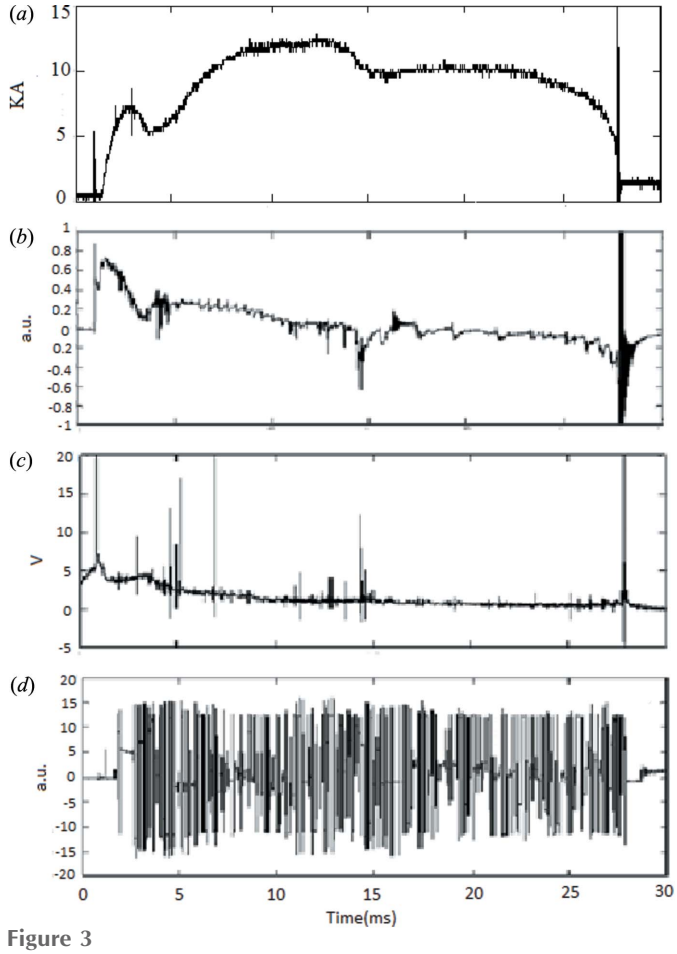

Figure 3
(*a*) Plasma current, (*b*) Mirnov oscillations, (*c*) loop voltage and (*d*) hard X-rays with respect to the time after decreasing the toroidal electric field.

In addition, the effects of the change in toroidal magnetic field on the runaway electrons transport have been presented. The plasma current, poloidal beta, hard X-ray intensity, Mirnov oscillation and loop voltage for the two discharges with the same conditions and only a change in the toroidal magnetic field are shown in Fig. 6. In this figure the toroidal magnetic field at the time of maximum plasma current is 0.441 T and 0.510 T for the blue and red curves, respectively. A detailed comparison of Figs. 6(*c*) and 6(*d*) reveals that an increase in the toroidal magnetic field can result in a decrease in intensity of magnetohydrodynamic (MHD) oscillations and an increase in runaway electrons generation. Furthermore, we analyzed the Mirnov signals obtained from Fig. 6(*d*) using the wavelet transform. In Fig. 7, wavelet spectra of the MHD oscillation are illustrated. Figs. 7(*a*) and 7(*b*) are related to the blue and red curves, respectively, in Fig. 6(*d*). As illustrated, an increase in the toroidal magnetic field resulted in a decrease in the frequency activity of the MHD oscillation.

The diffusion of runaway electrons for B_t = 0.405 T, 0.441 T, 0.510 T and 0.563 T is shown in Fig. 8. According to this figure, increasing the toroidal magnetic field causes a decrease in runaway electrons diffusion. In Fig. 8, the decrease of the runaway electrons diffusion by increasing the toroidal

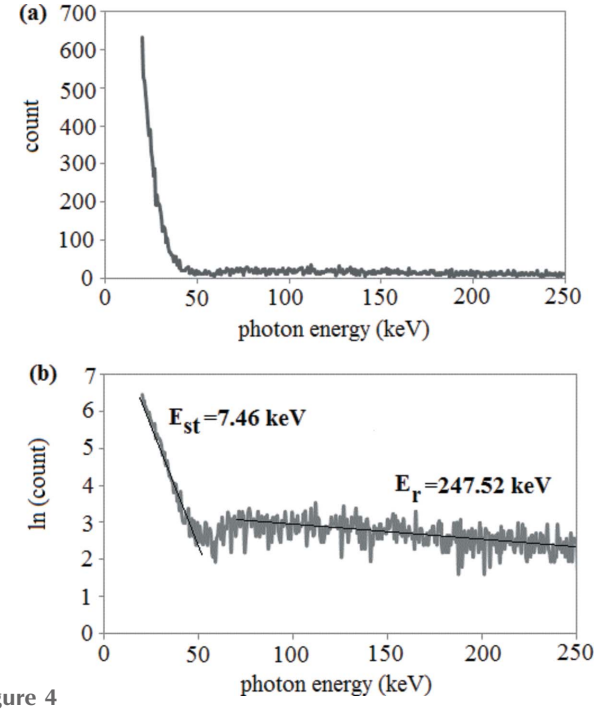

Figure 4
Hard X-ray emission energy spectra during the first 5 ms after the beginning of the plasma (*a*) and before decreasing the toroidal electric field (*b*).

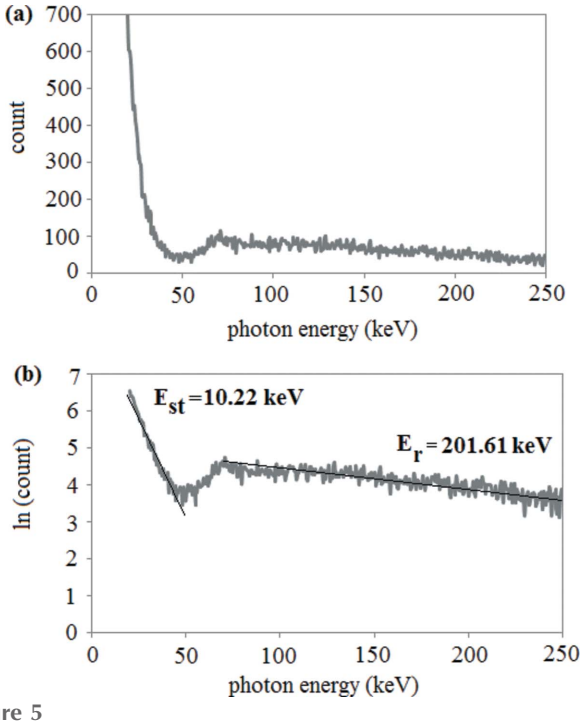

Figure 5
Hard X-ray emission energy spectra during the first 5 ms after the beginning of the plasma (*a*) and after decreasing the toroidal electric field (*b*).

magnetic field may be due to the decrease of magnetic turbulence. In Fig. 7, a comparison of the wavelet spectra (*a*) and (*b*) shows that increasing the toroidal magnetic field causes a decrease in MHD oscillation. According to equations (7) and (8) of Salar Elahi & Ghoranneviss (2009*a*) the increased magnetic turbulence increases the runaway electrons diffusion.

4. Summary and conclusions

In this paper the mean energy of runaway electrons before and after toroidal electric field changes was obtained by hard X-ray spectroscopy. The plasma current, loop voltage, Mirnov and hard X-ray intensity in both fields were measured. In addition, the effect of the change in the toroidal magnetic field on runaway electrons transport was considered. The results show that increasing the toroidal electric field will lead to more runaway electrons being generated and, in the same way, increasing the toroidal magnetic field causes a decrease in intensity of MHD oscillations and consequently more runaway electrons generated which is not good for plasma confinement and the chamber wall.

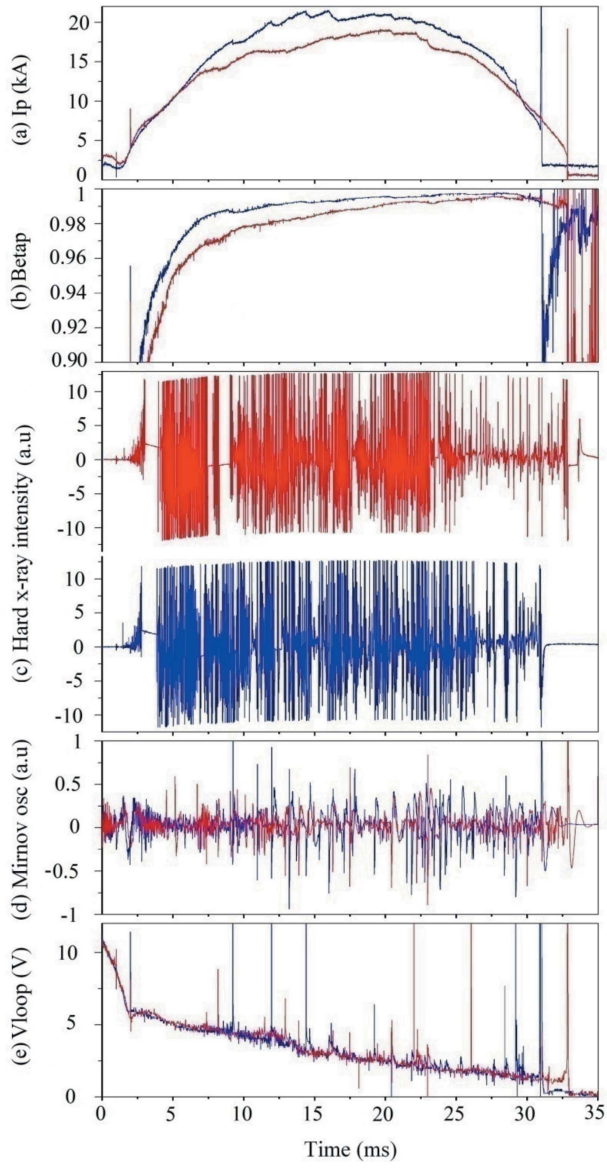

Figure 6
Time evolution of (*a*) plasma current, (*b*) poloidal beta, (*c*) hard X-ray intensity, (*d*) Mirnov oscillation and (*e*) loop voltage for the two toroidal magnetic fields B_t = 0.441 T and B_t = 0.510 T for the blue and red curves, respectively.

References

Cohen, R. H. (1979). *Phys. Fluids*, **19**, 239.
Connor, J. W. & Hastie, R. J. (1975). *Nucl. Fusion*, **15**, 415–424.
Emami, M., Ghoranneviss, M., Salar Elahi, A. & Rahimi Rad, A. (2009). *J. Plasma Phys.* **76**, 67–74.
Ghanbari, K., Ghoranneviss, M., Salar Elahi, A. & Saviz, S. (2014). *J. X-ray Sci. Technol.* **22**, 777–783.
Ghanbari, M. R., Ghoranneviss, M., Salar Elahi, A., Mohammadi, S. & Arvin, R. (2016). *J. Fusion Energy*, **35**, 180–186.
Ghoranneviss, M., Salar Elahi, A., Mohammadi, S. & Arvin, R. (2010). *Phys. Scr.* **82**, 035502.
Guan, X., Qin, H. & Fisch, N. J. (2010). *Phys. Plasmas*, **17**, 092502.
Gurevich, A. V. (1961). *Sov. Phys. JETP*, **12**, 904.
Helander, P., Erikson, L. G. & Anderson, F. (2002). *Plasma Phys. Contrib. Fusion*, **44**B, 247–262.
Jaspers, R., Finken, K. H., Mank, G., Hoenen, F., Boedo, J. A., Cardozo, N. J. L. & Schuller, F. C. (1993). *Nucl. Fusion*, **33**, 1775.
Kruskal, M. D. & Bernstein, I. B. (1962). PPPL Report MATT-Q-20, p. 174. Princeton Plasma Physics Laboratory, Princeton New Jersey, USA.
Lipa, M., Martin, G., Mitteau, R., Basiuk, V., Chatelier, M., Cordier, J. J. & Nygren, R. (2003). *Fusion Eng. Des.* **66–68**, 365–369.
Mikaili Agah, K., Ghoranneviss, M. & Salar Elahi, A. (2015*a*). *J. X-ray Sci. Technol.* **23**, 267–274.

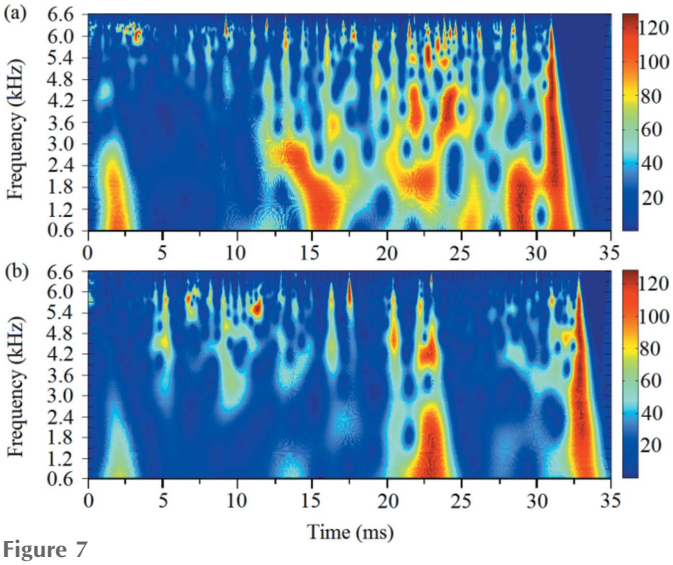

Figure 7
Wavelet spectrum showing the time evolution of the spectral properties of MHD activity. (*a*) Related to the blue curve and (*b*) related to the red curve in Fig. 6(*d*).

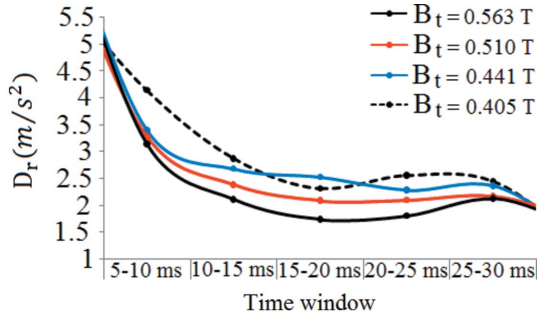

Figure 8
Time evolution of the diffusion of runaway electrons for B_t = 0.405 T (black dashed line), B_t = 0.441 T (blue line), B_t = 0.510 T (red line) and B_t = 0.563 T (black line).

Mikaili Agah, K., Ghoranneviss, M. & Salar Elahi, A. (2015*b*). *J. Inorg. Organomet. Polym. Mater.* **25**, 848–854.
Naghidokht, A., Khodabakhsh, R., Salar Elahi, A. & Ghoranneviss, M. (2016). *Fusion Eng. Des.* **107**, 82–89.
Rahimi Rad, A., Ghoranneviss, M., Emami, M. & Salar Elahi, A. (2009). *J. Fusion Energy*, **28**, 420.
Salar Elahi, A. & Ghoranneviss, M. (2009*a*). *Phys. Scr.* **80**, 045501.
Salar Elahi, A. & Ghoranneviss, M. (2009*b*). *J. Fusion Energy*, **28**, 416.
Salar Elahi, A. & Ghoranneviss, M. (2009*c*). *J. Fusion Energy*, **28**, 408.
Salar Elahi, A. & Ghoranneviss, M. (2009*d*). *J. Fusion Energy*, **28**, 412.
Salar Elahi, A. & Ghoranneviss, M. (2009*e*). *J. Fusion Energy*, **28**, 394.
Salar Elahi, A. & Ghoranneviss, M. (2009*f*). *J. Fusion Energy*, **28**, 404.
Salar Elahi, A. & Ghoranneviss, M. (2010*a*). *IEEE Trans. Plasma Sci.* **38**, 181–185.
Salar Elahi, A. & Ghoranneviss, M. (2010*b*). *IEEE Trans. Plasma Sci.* **38**, 3163–3167.
Salar Elahi, A. & Ghoranneviss, M. (2010*c*). *Fusion Eng. Des.* **85**, 724–727.
Salar Elahi, A. & Ghoranneviss, M. (2010*d*). *Phys. Scr.* **81**, 055501.
Salar Elahi, A. & Ghoranneviss, M. (2010*e*). *Phys. Scr.* **82**, 025502.
Salar Elahi, A. & Ghoranneviss, M. (2010*f*). *J. Fusion Energy*, **29**, 1–4.
Salar Elahi, A. & Ghoranneviss, M. (2014). *J. Fusion Energy*, **33**, 242–251.
Salar Elahi, A., Ghoranneviss, M. & Emami, M. (2009*b*). *J. Fusion Energy*, **28**, 385.
Salar Elahi, A., Ghoranneviss, M., Emami, M. & Rahimi Rad, A. (2009*a*). *J. Fusion Energy*, **28**, 346.
Salar Elahi, A., Ghoranneviss, M. & Rahimi Rad, A. (2009*c*). *J. Fusion Energy*, **28**, 390.
Sokolov, Yu. A. (1979). *JETP Lett.* **29**, 218.